Simulating Urban Growth for Baltimore-Washington Metropolitan Area by Coupling SLEUTH Model and Population Projection

Suwen Zhao

Thesis submitted to the faculty of the Virginia Polytechnic Institute and State University in partial fulfillment of the requirements for the degree of

Master of Science

In

Geography

Yang Shao. Chair
James B. Campbell. Member
Stephen Prisley. Member

04/16/2015
Blacksburg, Virginia

Key words: urban simulation model, SLEUTH, land use and land cover, population projection

Simulating Urban Growth for Baltimore-Washington Metropolitan Area by Coupling SLEUTH Model and Population Projection

Suwen Zhao

Abstract

This study used two modelling approaches to predict future urban landscape for the Baltimore-Washington metropolitan areas. In the first approach, we implemented traditional SLEUTH urban simulation model by using publicly available and locally-developed land cover and transportation data. Historical land cover data from 1996, 2001, 2006, and 2011 were used to calibrate SLEUTH model and predict urban growth from 2011 to 2070. SLEUTH model achieved 94.9% of overall accuracy for a validation year of 2014. For the second modelling approach, we predicted future county-level population (e.g., 2050) using historical population data and time-series forecasting. We then used future population projection of 2050, aided by strong population-imperviousness statistical relationship (R^2, 0.78-0.86), to predict total impervious surface area for each county. These population-predicted total impervious surface areas were compared to SLEUTH model output, at the county-aggregated spatial scale. For most counties, SLEUTH generated substantially higher number of impervious pixels. An annual urban growth rate of 6.24% for SLEUTH model was much higher than the population-based approach (1.33%), suggesting a large discrepancy between these two modelling approaches. The SLEUTH simulation model, although achieved high accuracy for 2014 validation, may have over-predicted urban growth for our study area. For population-predicted impervious surface area, we further developed a lookup table approach to integrate SLEUTH out and generated spatially explicit urban map for 2050. This lookup table approach has high potential to integrate population-predicted and SLEUTH-predicted urban landscape, especially when future population can be predicted with reasonable accuracy.

Contents:

List of Figures:

List of Tables:

Introduction

Land transformations from cultivated lands, forests and other natural lands to urban are typically irreversible and may lead to many ecosystem service related problems such as deterioration of water and air quality (Kalnay 2003), disruption of hydrological systems (Arnold and Gibbons 1996, Brun and Band 2000), loss of biodiversity (McKinney 2002), spread of invasive species (Alston and Richardson 2006), and forest/habitat fragmentation (Civco, Hurd et al. 2002, Radeloff, Hammer et al. 2005). Although urban built-up or impervious surface area may only account for a small fraction (e.g., less than 1 percent, (Angel, Sheppard et al. 2005)) of global land area, many researchers suggest that urban expansion into natural lands has far-reaching and disproportionate effects on mass, energy, and resource fluxes (Weng 2001). Urban built-up area in the US increased from 2.5% in 1990 to 3.1% in 2000 (Nowak and Walton 2005). In addition to area expansion, residential and commercial land developments at the periphery of urban areas often follow a low density and inefficient urban sprawl form (Song and Zenou 2006). Urban sprawl is one of main concerns for many US cities because it contributes to long commutes (Brueckner 2000), air pollution (Stone and Norman 2006), public health (Frumkin 2002), decay of downtown areas and a reduction in social interactions (Brueckner 2000).

Increasing awareness of urban growth and urban sprawl importance leads to many research efforts in monitoring and predicting urban growth patterns. For urban growth monitoring, remote sensing techniques are now routinely used for producing urban maps at local, regional, and national scales (Ridd 1995, Yuan and Bauer 2007, Jin, Yang et al. 2013). For example, the US National Land Cover Database (NLCD) provides ready-to-use sub-pixel impervious surface map (30 m resolution) every 5-6 years and the most recent one is for 2011 (Homer, Dewitz et al. 2007, Jin, Yang et al. 2013). In the same time, a large number of urban growth models have been

developed for simulating growth rates/patterns, understanding driving forces, and assessing urban growth consequences (Clarke and Gaydos 1998, Herold, Goldstein et al. 2003). Specific urban growth modelling approaches include regression and trend analysis (Nowak and Walton 2005), spatial logistic regression (Allen and Lu 2003, Cheng and Masser 2003, Hu and Lo 2007), geographically weighted logistic regression (Luo and Wei 2009), Cellular Automata (CA) (Clarke and Gaydos 1998, Li and Yeh 2000, Herold, Goldstein et al. 2003, Furtado, Ettema et al. 2012), and Agent-Based Models (Batty 2009). There are also many variations within each modeling category. For example, Santé, Garcí a et al. (2010) reviewed 33 urban CA models and suggested that it is difficult to select a particular CA for urban planners or in a real-world application. In general, the selection of a simulation model is depending on data availability, urban change information desired (e.g., rates, spatial patterns, from-to information), users' experiences of computer modelling, and consideration on computational complexity.

Among various CA simulation models, SLEUTH (Slope, Land use, Excluded, Urban, Transportation and Hillshade) model is probably one of the most widely used due to its simplicity and intuitiveness (Clarke, Gazulis et al. 2007, Santé, Garcí a et al. 2010, Furtado, Ettema et al. 2012). Within SLEUTH framework, urban spaces are represented as a grid of cells that can change states (e.g., urban and non-urban) as the model iterates. The state of each cell is depending on its current state and neighboring cells' states. Using historical land cover maps, transportation layers, a digital elevation model (DEM), and a map of areas excluded from urbanization as model inputs, SLEUTH approximates spatial-temporal patterns of urban development by calibrating five parameters: dispersion, breed, spread, slope and road gravity (Clarke and Gaydos 1998). An inventory of SLEUTH applications is provided by (Clarke, Gazulis et al. 2007). Most previous published studies focused on model calibration for improving

prediction (Silva and Clarke 2002), or coupling SLEUTH with other bio-physical models to assess potential impacts from urban expansion (Yang and Lo 2003).

Data availability and data quality are main challenges for SLEUTH model. SLEUTH cannot learn historical urban growth patterns if input land cover (or transportation) maps have large inconsistency. Model calibration is another difficult task since many possible parameter combinations need to be examined and the goodness of fit measures vary significantly in published studies (Clarke and Gaydos 1998, Silva and Clarke 2002). Furthermore, some key drivers of urban expansion, population as one example, are not directly incorporated in SLEUTH simulation model. In general, a county with fast population growth would expect more urban development, while a county with relatively stable population may experience slower urban development. Population data, however, are often provided at census block or block group scale. The lack of spatially explicit population data (e.g., pixel level) may limit their direct linkage to SLEUTH simulation.

At the census block group or county spatial scales, previous research shows strong positive relationships between population and urban built-up areas (Lo 1986, Harvey 2003, Lo and Quattrochi 2003, Li and Weng 2005). Intuitively, future population projection (e.g., 2050) at county level (or other spatial unit) may be used for predicting total built-up area for a future time period. Recent advances in population projection have shown great potential in providing US county-level population data for years 2030 and 2050 (McKee, Rose et al. 2015). This type of population projection, aided by population-built-up statistical relationship, may provide an alternative approach to predict total built-up area at selected spatial analytical unit. The population-predicted built-up area can serve as a reference or be compared with spatially aggregated results from SLEUTH simulation model. One limitation of population-predicted

urban map is lack of spatial detail (e.g., county level vs. pixel level). Few previous published studies have examined redistributing total built-up area to pixel (e.g., 90m resolution) within the spatial analytical unit.

The overall objective of this study was to simulate future urban development for the Baltimore-Washington metropolitan area using SLEUTH model and population projection. Specific research tasks include: (1) implement SLEUTH model with high quality land cover and transportation maps; (2) construct county-level population projection for 2050 and use population-impervious surface relationship to estimate county-level total impervious surface area in 2050; (3) compare population-derived impervious surface area and SLEUTH output for 2050, at county-level; and (4) Distribute population-derived total impervious surface area of 2050 to pixel-scale by coupling SLEUTH simulation output. The resultant 2050 urban map was then compared to the current NLCD map (2011) to determine the "from-to" land change information and landscape fragmentation for the Baltimore-Washington metropolitan area.

Study Area

The Baltimore-Washington metropolitan (BWM) area includes two US major cities: Baltimore, Maryland and Washington, D.C. It is the fourth largest combined statistical area in the US, containing a total of 35 counties from Maryland, Northern Virginia, West Virginia, and Pennsylvania. In 2012, the BWM's total estimated population was 9,331,587, an increase of about 39% compared to 1990. Some BWM counties, such as Fairfax County and Loudoun County in Northern Virginia, are among the fastest-growing areas in the nation (Masek, Lindsay et al. 2000, Fuller 2001). Loudoun County's total population increased 150% from 1980 to current. In the last several decades, land cover change in the BWM region has been dominated

by conversion of prime agricultural land (or forest land) to moderate-to-low density impervious surfaces (Fuller 2001). Urban sprawl in this region has raised many concerns, especially on its impacts of water quality, forest fragmentation, and overall ecosystem services (Burchell, Shad et al. 1998, Grumet 2000, Fuller 2001, Jantz, Goetz et al. 2004). Policy makers, planners and researchers are particularly interested in the area's future population change, urban growth rates/patterns, and their potential environmental impacts (Jantz, Goetz et al. 2003). For this study, a rectangle shape (150km by 120km) was used to cover BWM's two major city centers and their sprawling suburban areas (Figure 1). This selected study area allowed us to model main urban growth patterns of BWM.

Methods

SLEUTH input data preparation

SLEUTH model requires four years' binary urban/non-urban maps to capture historical land cover information. The Multi-Resolution Land Characteristics Consortium (MRLC, http://www.mrlc.gov/) provides NLCD land cover data for 1992, 2001, 2006, and 2011. The 2001, 2006, and 2011 NLCD land cover data use consistent classification scheme and classification accuracies are reasonably high (Wickham, Stehman et al. 2010). These three NLCD data products follow a 5-year mapping interval. Each product also provides a 30m subpixel proportional impervious surface map, which can be easily recoded as urban/non-urban pixels for SLEUTH model input. However, the 1992 NLCD used a different land cover classification scheme/algorithm and it cannot be directly compared with the other three NLCD data layers. To maintain temporal (e.g., ~ 5 years) and thematic consistency of land cover input data for SLEUTH model, we locally developed a 1996 subpixel proportional impervious surface map using a 1996 Landsat TM image. We followed image analytical method of Xian, Homer et al. (2009) to generate the 1996 urban map. Specifically, we first used a pair of Landsat TM images from 1996 and 2001 to identify the no-change pixels between the image pair trough simple image ratioing and thresholding (Singh 1989). The no-change pixels were assumed to have the same subpixel proportional impervious surface between 1996 and 2001. Since the 2001 subpixel proportional impervious surface map is available through NLCD 2001, we were able to select training pixels within the 'no-change' area and establish relationships between Landsat TM (1996) signals and subpixel proportional impervious surface. A total of over 40,000 training pixels were randomly selected. We used a neural network algorithm to approximate the spectral-imperviousness relationship (Shao and Lunetta 2011, Shao and Lunetta 2012). The trained neural

network was then applied to the entire 1996 Landsat image to generate subpixel proportional impervious surface map. This locally developed 1996 impervious surface map and three NLCD impervious surface maps (2001, 2006, and 2011) were rescaled to 90-m spatial resolution to reduce computational cost of SLEUTH (Clarke and Gaydos 1998). By spatial aggregation, errors of image co-registration can also be reduced. A threshold of 40% subpixel imperviousness was used to convert all proportional impervious surface maps to binary urban/non-urban land cover layers.

A 30m digital elevation model (DEM) was obtained from the USGS NationalMap Viewer and Download Platform (http://nationalmap.gov/viewer.html). Slope and hillshade layers were generated from the 30m DEM dataset. The primary transportation layer (TIGER 2010) was obtained from the United States Department of Agriculture's Geospatial Data Gateway (http://datagateway.nrcs.usda.gov/). An overlay of the 2010 TIGER primary roads on top of 1996, 2001, and 2006 Landsat images allowed us to manually update (mainly deleting road segments) the transportation layer for 1996, 2001, and 2006, respectively. Four years' transportation layers were then converted to binary raster format for SLEUTH input. All input raster layers were converted to Graphics Interchange Format (GIF) before running the SLEUTH model.

SLEUTH Model calibration, prediction, and accuracy assessment

SLEUTH calibration relies on 5 model parameters (dispersion, breed, spread, slope, and road gravity) and their various combinations. The basis of SLEUTH calibration is to conduct a grid searching to find a best 5-coefficent combination to capture historical land cover change patterns (Clarke and Gaydos 1998, Silva and Clarke 2002, Jantz, Goetz et al. 2003). Given user-defined initial coefficient values and incremental steps, SLEUTH model automatically test all possible

parameter combinations for 'brute force' Monte Carlo runs. For each combination, the total urban pixels and spatial patterns were compared with historical land cover data to calculate fit statistics (e.g., r^2 statistics, edges, spatial match, etc.). The best performing coefficient values can then be used for urban growth prediction. We followed Jantz, Goetz et al. (2003) study to use maximum parameter value range of 1-100, increment step of 25, and 100 Monte Carlo iterations. The final coefficient-combination was selected when simulation results matched well with the 2011 urban map, in terms of total urban pixel numbers (Jantz, Goetz et al. 2003). This set of coefficients was then used to simulate urban growth from 2011 to 2070.

It should be noted that a well-calibrated SLEUTH model only means that the model could capture the historical urban change rates (in some cases, spatial patterns). The selection of best coefficients is also depending on a user-defined goodness of fit measure, which does not indicate a successful simulation for future land change. To further evaluate the accuracy of our SLEUTH model, we used a 2014 urban map as an independent dataset to assess SLEUTH predictive performance. The 2014 urban map was derived from a Landsat 8 image using the same sub-pixel impervious surface mapping techniques described above. SLEUTH model accuracy assessment was conducted at two levels. For the first level, we simply compared the total urban pixels from SLEUTH model prediction for year 2014 and the actual 2014 urban map. The second level of comparison was conducted at pixel-scale. We used a standard error matrix (Congalton 1991) to summarize the agreements between SLEUTH predicted map and actual urban map derived from the 2014 Landsat 8 image. Overall accuracy and kappa coefficient were calculated as accuracy statistics.

Population projection

We used county-level time-series population data from 1990 to 2010 to project population for year 2050. For all counties within the study area, annual population data from 1990 to 2010 were obtained from the United States Census Bureau. Initial population trend analysis suggested that population has been increasing in relatively smooth trends for almost all counties. For each county, simple liner exponential smoothing method was used to fit the time-series population data and predict annual population from 2010 to 2050. For District of Columbia, preliminary time-series data analysis suggested large fluctuation (i.e., decrease and then increase). We used an Autoregressive integrated moving average (ARIMA) model to produce population forecasting for this special case.

Population-imperviousness relationship and county-level total impervious surface area prediction for year 2050

Previous published studies suggest that there are strong positive relationships between population and impervious surface area and many researchers have used impervious surface map to estimate population at census block group or county scales (Lo 1986, Harvey 2003, Lo and Quattrochi 2003, Li and Weng 2005, Lu, Weng et al. 2006). Similarly, we hypothesize that total impervious surface area for each county can be estimated from county-level population if there is a simple and strong linear relationship between the two variables.

We examined county-level population-imperviousness relationship using historical land cover data and population statistics for 1996, 2001, 2006, and 2011. We generated regression line between these two variables for each study year:

$$Y = a + bX$$

where Y is the total impervious surface area for each county, X is total population for each county, a and b are intercept and slope for simple regression. If regression lines are similar for historical time-periods (e.g, 1996 – 2011), we may use the same statistical relationship and population projection to estimate total impervious surface area for each county, for a future time period (e.g., 2050). We define this impervious surface area estimation as population-predicted impervious surface. For each county, we only have a number summarizing total impervious surface area, thus it is not spatially explicit (e.g., county vs. SLEUTH's pixels).

Compare and couple SLEUTH simulated and population-predicted impervious surface area for 2050

For year 2050, we summarized SLEUTH predicted impervious surface pixels for each county and compared to the population-predicted impervious area using scatter plots. R^2 and RMSE values were also calculated to assess the agreement between two predictions. For population-predicted county-scale impervious surface numbers, we designed a lookup table approach to distribute total impervious surface area of 2050 to pixel-scale by coupling SLEUTH simulation output. Specifically, for any study county, we first generated SLEUTH-based look-up table of total impervious surface area from 2020 to 2070. We then compared the population-predicted total impervious surface area for 2050 with the look-up table to find the closest matching value (e.g., SLEUTH output 2040 or any year from 2020-2070). The specific spatial extents/patterns for the matching year (e.g., SLEUTH output 2040) were then used to represent the actual spatial distribution of impervious surface pixels for year 2050. This look-up table approach was repeated for all study counties, independent to each other. This coupling approach assumed that population projection and population-predicted total impervious surface area are reasonably

accurate. The SLEUTH outputs are useful in determining urban spatial patterns, since urban expansion may still follow rules controlled by historical land use, transportation, and elevation.

Urban growth and spatial pattern analysis

The final 2050 urban map, or population-SLUETH coupled output, was compared to the 2011 NLCD map to analyze land change and landscape pattern dynamics. The FRAGSTATS (MCGARIGAL and Marks 1995) software package was used to quantify landscape patterns and their changes for the study area. The FRAGSTATS has been widely used in landscape ecology and land fragmentation analysis (Reed, Johnson-Barnard et al. 1996, Keleş, Sivrikaya et al. 2008). Among various pattern indices calculated by FRAGSTATS, we selected five commonly used measurements to characterize spatial patterns of impervious surface area: (1) the total number of patches, (2) the mean patch size, (3) the largest patch index, (4) edge density and (5) the Perimeter-Area Fractal Dimension.

Results and Discussion

Accuracy assessment of SLEUTH model

SLEUTH output for year 2014 was compared to the actual 2014 urban/non-urban map derived from the Landsat 8 image. For the entire study area, the ratio between SLEUTH predicted and Landsat-derived total urban pixels was 0.943. This ratio suggests that SLEUTH under-estimated total impervious surface area for year 2014. For pixel-by-pixel comparison, Table 1 shows error matrix by using Landsat-derived map as reference. The overall accuracy was 94.9%. The high level of overall accuracy can be misleading because a majority of pixels in the study area were non-urban pixels and most remained as non-urban through time. This relatively stable non-urban class had very high user's (97.0%) and producer's accuracy (97.5%), thus inflated overall accuracy. For urban class, about 69.7% of SLEUTH predicted urban pixels were actual urban pixels labeled by 2014 reference map. Meanwhile, only 65.8% of actual urban pixels were correctly predicted by SLEUTH model.

Following Jantz's (Jantz, Goetz et al. 2003) research, we also conducted accuracy assessment for areas where changes were observed or predicted (Table 2). The overall accuracy reduced to 46.1%, suggesting relatively low predictive capability of SLEUTH model with regard to urban pixel locations and spatial patterns. We note that Jantz's (Jantz, Goetz et al. 2003) work achieved 19% overall accuracy for the same study area even after rigorous SLUETH model calibration. Therefore, our SLEUTH model output was still acceptable, since we used an independent validation dataset (2014 Landsat-derive map) for our accuracy assessment.

Population projection for 2050

Figure 2 shows an example of linear exponential smoothing model for population projection of Montgomery County, Maryland. This county experienced a linear population growth from 1990 to 2010 and growth rate was relatively stable over time. The linear exponential smoothing model resulted a R^2 value of 0.99, suggesting good model fit for historical time-series population data. Most counties in the study area followed the similar population change trajectory and R^2 values were in the range of 0.56 ~ 0.99. Figure 3 shows District of Columbia's population change pattern and future projection. DC's population decreased from 1990 to 2000 and then has been steadily increasing. An ARIMA model appeared to be effective for approximating population trends for the district. Figure 4a shows predicted total population for each county in 2050. The BWM area will have a total population of 13,813,628 by 2050, a 56.52% of increase compared to 2010. Fairfax County will have a total population of 1,950,783, remaining as the most populous county in Virginia. Figure 4b shows R^2 values of time-series models. Relatively low R^2 values were observed for District of Columbia and two counties at the edge of the study area.

Population-imperviousness relationship

Strong linear relationships were observed between county-level total impervious surface area and population statistics for years 1996, 2001, 2006 and 2011 (Figure 5). Simple linear regression models generated R^2 values of 0.86, 0.84, 0.68 and 0.78 for four years, respective. More importantly, two linear regression lines for 2006 and 2011 have almost identical intercept and slope values, suggesting relatively consistent population-imperviousness relationship at the county-level. The regression model for 2011 is:

Impervious surface area = 1008.89 + 0.0156*population

We used the above regression model and population projection in 2050 to estimate total impervious surface area for each county in 2050. Figure 6 compares population-derived impervious area to SLEUTH output for year 2050. For most counties, SLEUTH predicted impervious areas were substantially higher than those estimated from population projection. For example, SLEUTH predicted 90.92 km^2 of impervious surface area for Stafford County, while population-derived number was 40.06 km^2.

Distribute population-derived total impervious surface area to pixel-scale

For simplicity, we used one county, Stafford County, Virginia, as an example to illustrate our lookup table and impervious surface area distribution results. For this county, population-derived total impervious surface area is around 40km^2 for year 2050. For the same county, figure 7 shows SLEUTH predicted impervious surface area from 2011 to 2070. The total impervious surface area increased from about 20 km^2 to 115 km^2 for the simulation period. Based on the urban growth curve (Figure 7) or a lookup table approach, the nearest matching value for population-predicted total impervious surface area was from SLEUTH output for year 2028. Therefore, we selected 2028 SLEUTH output as the 2050 population-predicted urban map, in a spatially explicit manner. Figure 8 essentially compares spatial patterns of impervious surface maps from SLEUTH-predicted and population-predicted approaches for year 2050. SLEUTH predicted 2050 impervious surface map has much larger and square-shaped blocks compared to population-predicted maps. Figure 9 compares a NLCD 2011 impervious surface map, SLUETH-simulated 2050 map, and population-predicted 2050 map. Clearly the population-predicted 2050 map has less impervious surface area compared to initial SLEUTH prediction. Neither map can be considered more accurate than the other, since model validation cannot be conducted for both maps. However, the SLUETH predicted 2050 map has an annual urban

growth rate of 6.24% compared to the 2011 impervious surface area from NLCD. The population-predicted 2050 urban map, on the other hand, has an annual urban growth rate of 1.33% compared to 2011.

Land change and Landscapes spatial pattern analysis

The population-predicted 2050 impervious surface map was compared with the 2011 NLCD map to analyze changes in land cover (Table 3 and figure 10) and landscape patterns. In addition to stable urban2011-urban2050 class (59.1%), we found that a significant portion (32.1%) of 2050 impervious surface pixels were converted from low density developed lands (e.g., <40% impervious surface area within 90m pixel) in 2011. This finding was not surprising since these low density developed lands are most often located at urban edges or suburban areas and they are more likely to be converted to high density urban. About 4.5% of new impervious surface areas in 2050 come from forest class of 2011. Agriculture lands will contribute less than 2% of the total urban areas in 2050.

Selected landscape pattern indices were calculated to further quantify spatial patterns of impervious surface cover and their dynamics (Table 4). Total impervious surface area was predicted to increase from 105537 hectares in 2011 to 174973 hectares in 2050. Total impervious surface patch number will decrease from 12013 in 2011 to 8402 in 2050. Accordingly, mean patch size will increase from 8.79 to 20.56 hectares. Largest urban patch index will increase 4 times during next decades.

Conclusions

This study predicted future urban landscape for the Baltimore-Washington Metropolitan area using SLEUTH model, population projection, and coupling SLEUTH and population projection approaches. SLEUTH simulation was validated using an independent 2014 urban map derived from a Landsat 8 image. The overall accuracy was 94.9%, although individual urban class has much lower user's (69.7%) and producer's accuracies (65.8%). Future population (e.g., 2050) at county-scale was predicted using historical time-series population data. Strong linear relationship (R^2, 0.78-0.86) between population and imperviousness allowed us to estimate total impervious surface area at county-scale. We found that SLEUTH model predicted substantially higher total impervious surface area compared to population-derived numbers, although neither approach could be determined as more accurate. A lookup table method was developed to generate a more spatially explicit map for population-based simulation. If future population projection is reliable, the coupling of population projection and SLEUTH model would provide an effective method to generate detailed impervious surface map to assist other environmental and social research efforts.

Reference:

Allen, J. and K. Lu (2003). "Modeling and prediction of future urban growth in the Charleston region of South Carolina: a GIS-based integrated approach." Ecology and Society **8**(2): 2.

Alston, K. P. and D. M. Richardson (2006). "The roles of habitat features, disturbance, and distance from putative source populations in structuring alien plant invasions at the urban/wildland interface on the Cape Peninsula, South Africa." Biological Conservation **132**(2): 183-198.

Angel, S., et al. (2005). The dynamics of global urban expansion, World Bank, Transport and Urban Development Department Washington, DC.

Arnold, C. L., Jr. and C. J. Gibbons (1996). "Impervious surface coverage: The emergence of a key environmental indicator." American Planning Association. Journal of the American Planning Association **62**(2): 243.

Batty, M. (2009). "Urban modeling." International Encyclopedia of Human Geography. Oxford, UK: Elsevier.

Brueckner, J. K. (2000). "Urban sprawl: diagnosis and remedies." International regional science review **23**(2): 160-171.

Brun, S. E. and Band (2000). "Simulating runoff behavior in an urbanizing watershed." Computers, environment and urban systems **24**(1): 5.

Burchell, R. W., et al. (1998). The costs of sprawl-revisited.

Cheng, J. and I. Masser (2003). "Urban growth pattern modeling: a case study of Wuhan city, PR China." Landscape and urban planning **62**(4): 199-217.

Civco, D. L., et al. (2002). "Quantifying and describing urbanizing landscapes in the Northeast United States." Photogrammetric Engineering and Remote Sensing **68**(10): 1083-1090.

Clarke, K. C. and L. J. Gaydos (1998). "Loose-coupling a cellular automaton model and GIS: long-term urban growth prediction for San Francisco and Washington/Baltimore." International journal of geographical information science **12**(7): 699-714.

Clarke, K. C., et al. (2007). "A decade of SLEUTHing: Lessons learned from applications of a cellular automaton land use change model." Classics in IJGIS: twenty years of the international journal of geographical information science and systems: 413-427.

Congalton, R. G. (1991). "A review of assessing the accuracy of classifications of remotely sensed data." Remote Sensing of Environment **37**(1): 35-46.

Frumkin, H. (2002). "Urban sprawl and public health." Public health reports **117**(3): 201.

Fuller, D. O. (2001). "Forest fragmentation in Loudoun County, Virginia, USA evaluated with multitemporal Landsat imagery." Landscape Ecology **16**(7): 627-642.

Furtado, B. A., et al. (2012). "A cellular automata intraurban model with prices and income-differentiated actors." Environment and Planning-Part B **39**(5): 897.

Grumet, R. S. (2000). "Bay, plain, and piedmont: a landscape history of the Chesapeake heartland from 1.3 billion years ago to 2000." The Chesapeake Bay Heritage Context Project, Annapolis, Maryland.

Harvey, J. (2003). "Population estimation at the pixel level: developing the expectation maximization technique."

Herold, M., et al. (2003). "The spatiotemporal form of urban growth: measurement, analysis and modeling." Remote Sensing of Environment **86**(3): 286-302.

Homer, C., et al. (2007). "Completion of the 2001 national land cover database for the counterminous United States." Photogrammetric Engineering and Remote Sensing **73**(4): 337.

Hu, Z. and C. Lo (2007). "Modeling urban growth in Atlanta using logistic regression." Computers, environment and urban systems **31**(6): 667-688.

Jantz, C. A., et al. (2004). "Using the SLEUTH urban growth model to simulate the impacts of future policy scenarios on urban land use in the Baltimore-Washington metropolitan area." Environment and Planning B **31**(2): 251-272.

Jantz, C. A., et al. (2003). Mapping and modeling land use change in the Baltimore-Washington, DC Area: Tools for regional planning in the Chesapeake Bay watershed, USA.

Jin, S., et al. (2013). "A comprehensive change detection method for updating the National Land Cover Database to circa 2011." Remote Sensing of Environment **132**: 159-175.

Kalnay, E. (2003). "Impact of urbanization and land-use change on climate." Nature **423**(6939): 528-531.

Keleş, S., et al. (2008). "Urbanization and forest cover change in regional directorate of Trabzon forestry from 1975 to 2000 using landsat data." Environmental monitoring and assessment **140**(1-3): 1-14.

Li, G. and Q. Weng (2005). "Using Landsat ETM+ imagery to measure population density in Indianapolis, Indiana, USA." Photogrammetric Engineering & Remote Sensing **71**(8): 947-958.

Li, X. and A. G.-O. Yeh (2000). "Modelling sustainable urban development by the integration of constrained cellular automata and GIS." International journal of geographical information science **14**(2): 131-152.

Lo, A. Y. (1986). "Bayesian statistical inference for sampling a finite population." The Annals of Statistics: 1226-1233.

Lo, C. and D. A. Quattrochi (2003). "Land-Use and Land-Cover Change, Urban Heat Island Phenomenon, and Health Implications." Photogrammetric Engineering & Remote Sensing **69**(9): 1053-1063.

Lu, D., et al. (2006). "Residential population estimation using a remote sensing derived impervious surface approach." International journal of remote sensing **27**(16): 3553-3570.

Luo, J. and Y. D. Wei (2009). "Modeling spatial variations of urban growth patterns in Chinese cities: the case of Nanjing." Landscape and urban planning **91**(2): 51-64.

Masek, J., et al. (2000). "Dynamics of urban growth in the Washington DC metropolitan area, 1973-1996, from Landsat observations." International journal of remote sensing **21**(18): 3473-3486.

MCGARIGAL, K. M. and B. Marks (1995). "B.(1995)–FRAGSTATS: Spatial Pattern Analysis Program for Quantifying Landscape Structure." General Technical Report PNW-GTR-351. US Department of Agriculture, Forest Service, Pacific Northwest Research Station.

McKee, J. J., et al. (2015). "Locally adaptive, spatially explicit projection of US population for 2030 and 2050." Proceedings of the National Academy of Sciences: 201405713.

McKinney, M. L. (2002). "Urbanization, Biodiversity, and Conservation The impacts of urbanization on native species are poorly studied, but educating a highly urbanized human population about these impacts can greatly improve species conservation in all ecosystems." BioScience **52**(10): 883-890.

Nowak, D. J. and J. T. Walton (2005). "Projected urban growth (2000–2050) and its estimated impact on the US forest resource." Journal of Forestry **103**(8): 383-389.

Radeloff, V. C., et al. (2005). "The wildland-urban interface in the United States." Ecological applications **15**(3): 799-805.

Reed, R. A., et al. (1996). "Fragmentation of a forested Rocky Mountain landscape, 1950–1993." Biological Conservation **75**(3): 267-277.

Ridd, M. K. (1995). "Exploring a VIS (vegetation-impervious surface-soil) model for urban ecosystem analysis through remote sensing: comparative anatomy for cities†." International journal of remote sensing **16**(12): 2165-2185.

Santé, I., et al. (2010). "Cellular automata models for the simulation of real-world urban processes: A review and analysis." Landscape and urban planning **96**(2): 108-122.

Shao, Y. and R. S. Lunetta (2011). "Sub-pixel mapping of tree canopy, impervious surfaces, and cropland in the Laurentian Great Lakes Basin using MODIS time-series data." Selected Topics in Applied Earth Observations and Remote Sensing, IEEE Journal of **4**(2): 336-347.

Shao, Y. and R. S. Lunetta (2012). "Comparison of support vector machine, neural network, and CART algorithms for the land-cover classification using limited training data points." ISPRS Journal of Photogrammetry and Remote Sensing **70**: 78-87.

Silva, E. A. and K. C. Clarke (2002). "Calibration of the SLEUTH urban growth model for Lisbon and Porto, Portugal." Computers, environment and urban systems **26**(6): 525-552.

Singh, A. (1989). "Review article digital change detection techniques using remotely-sensed data." International journal of remote sensing **10**(6): 989-1003.

Song, Y. and Y. Zenou (2006). "Property tax and urban sprawl: Theory and implications for US cities." Journal of Urban Economics **60**(3): 519-534.

Stone, B. and J. M. Norman (2006). "Land use planning and surface heat island formation: A parcel-based radiation flux approach." Atmospheric Environment **40**(19): 3561-3573.

Weng, Q. (2001). "A remote sensing? GIS evaluation of urban expansion and its impact on surface temperature in the Zhujiang Delta, China." International journal of remote sensing **22**(10): 1999-2014.

Wickham, J., et al. (2010). "Thematic accuracy of the NLCD 2001 land cover for the conterminous United States." Remote Sensing of Environment **114**(6): 1286-1296.

Xian, G., et al. (2009). "Updating the 2001 National Land Cover Database land cover classification to 2006 by using Landsat imagery change detection methods." Remote Sensing of Environment **113**(6): 1133-1147.

Yang, X. and C. Lo (2003). "Modelling urban growth and landscape changes in the Atlanta metropolitan area." International journal of geographical information science **17**(5): 463-488.

Yuan, F. and M. E. Bauer (2007). "Comparison of impervious surface area and normalized difference vegetation index as indicators of surface urban heat island effects in Landsat imagery." Remote Sensing of Environment **106**(3): 375-386.

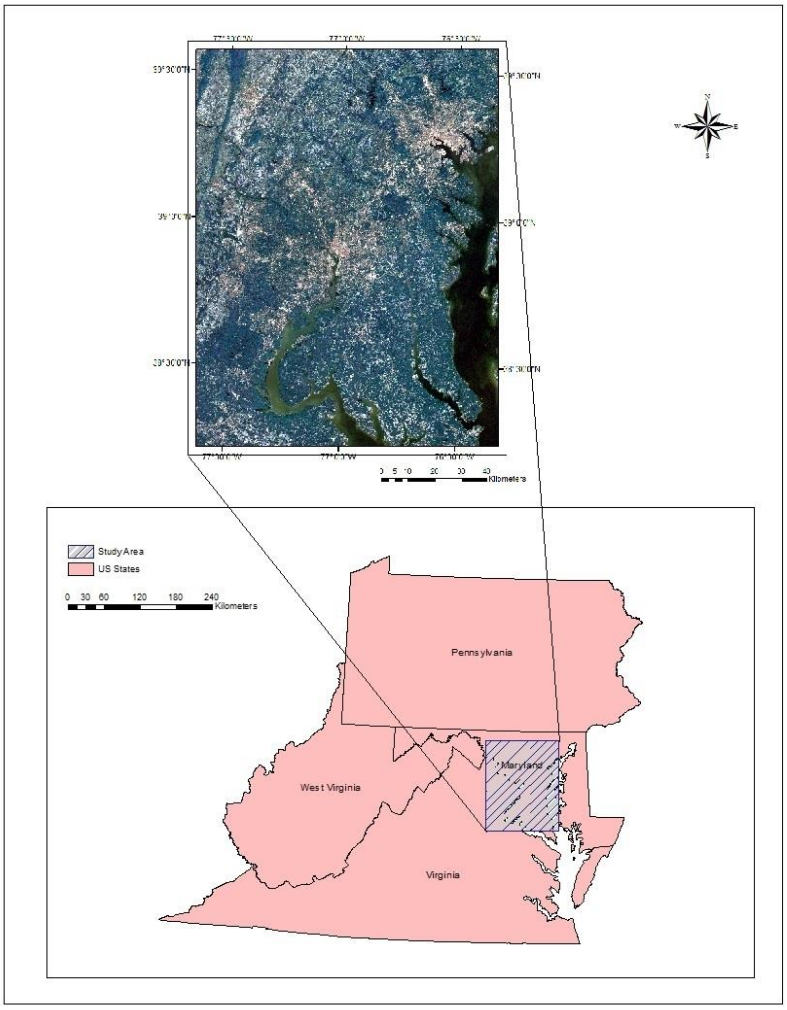

Figure 1. Study Area

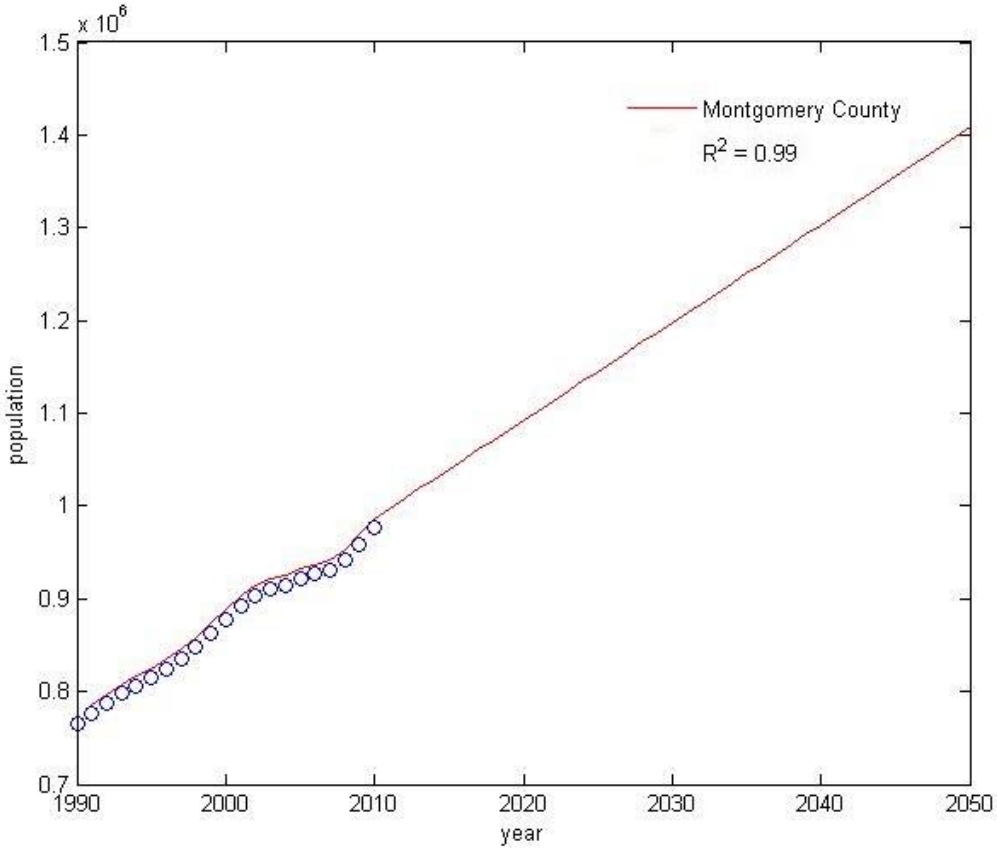

Figure 2. Time series predicted total population for Montgomery County from 1990 to 2050

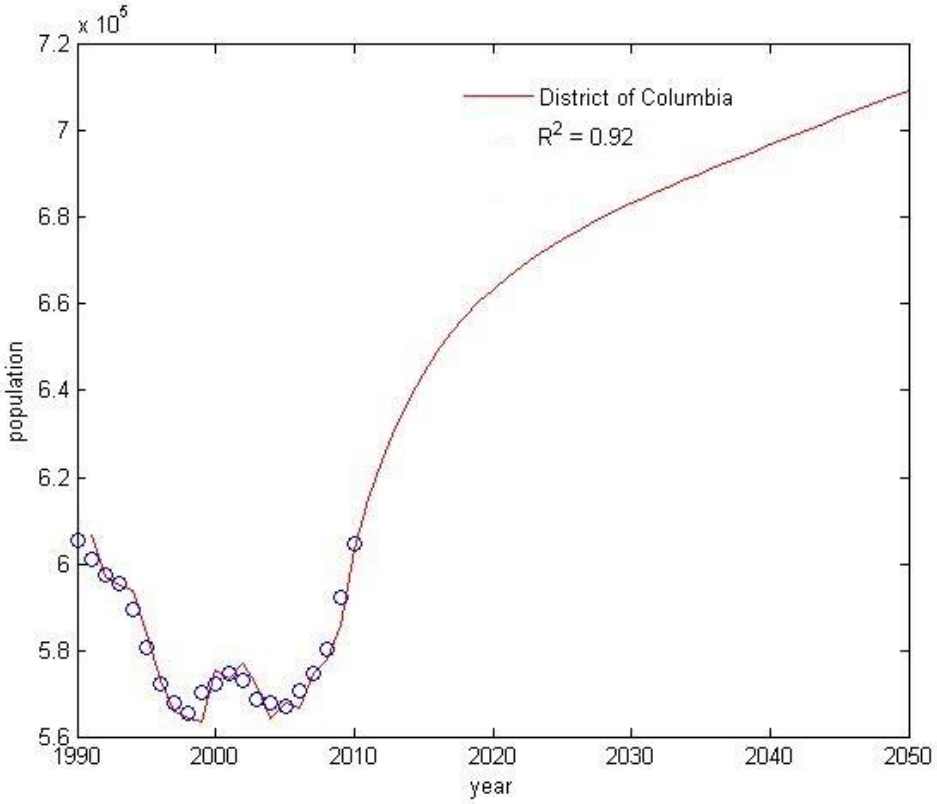

Figure 3. Time series predicted total population for District of Columbia from 1990 to 2050

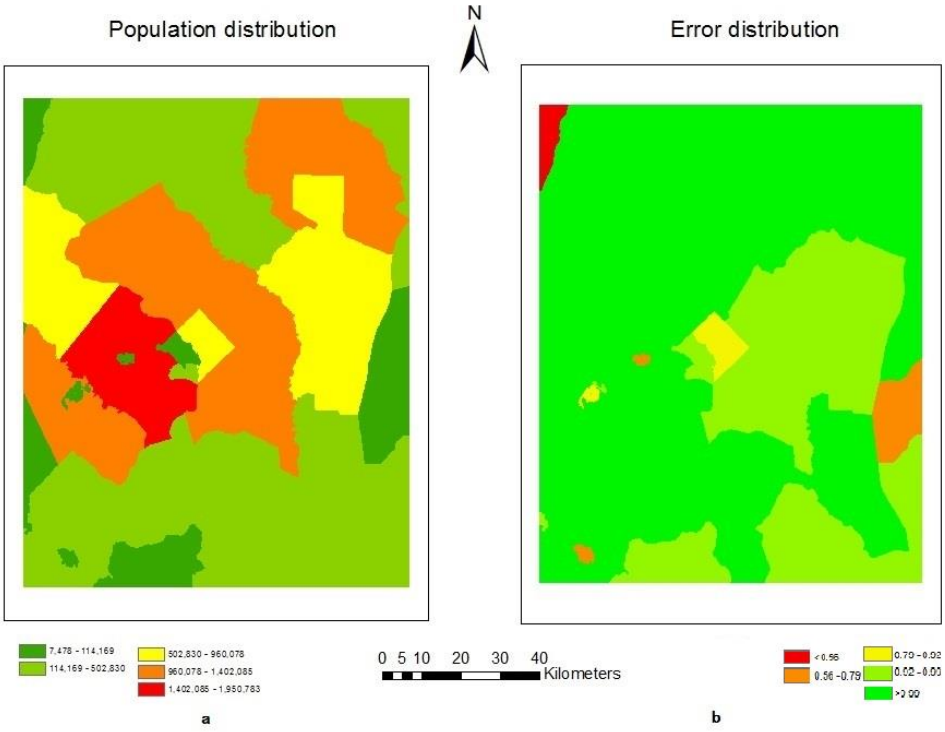

Figure 4. Population distribution (a) and Error distribution (b) in 2050 predicted by time series model

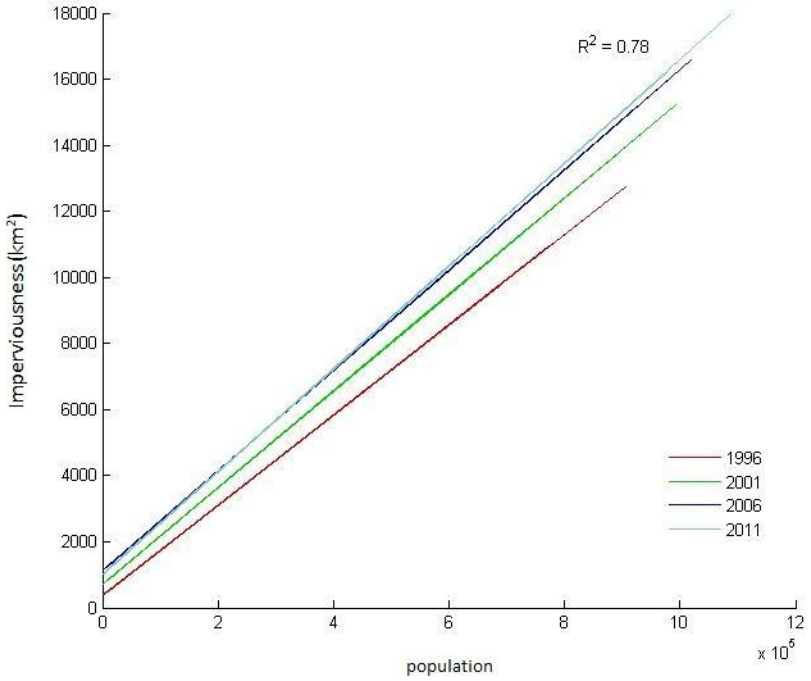

Figure 5. Linear relationship between imperviousness and population for 1996, 2001, 2006 and 2011

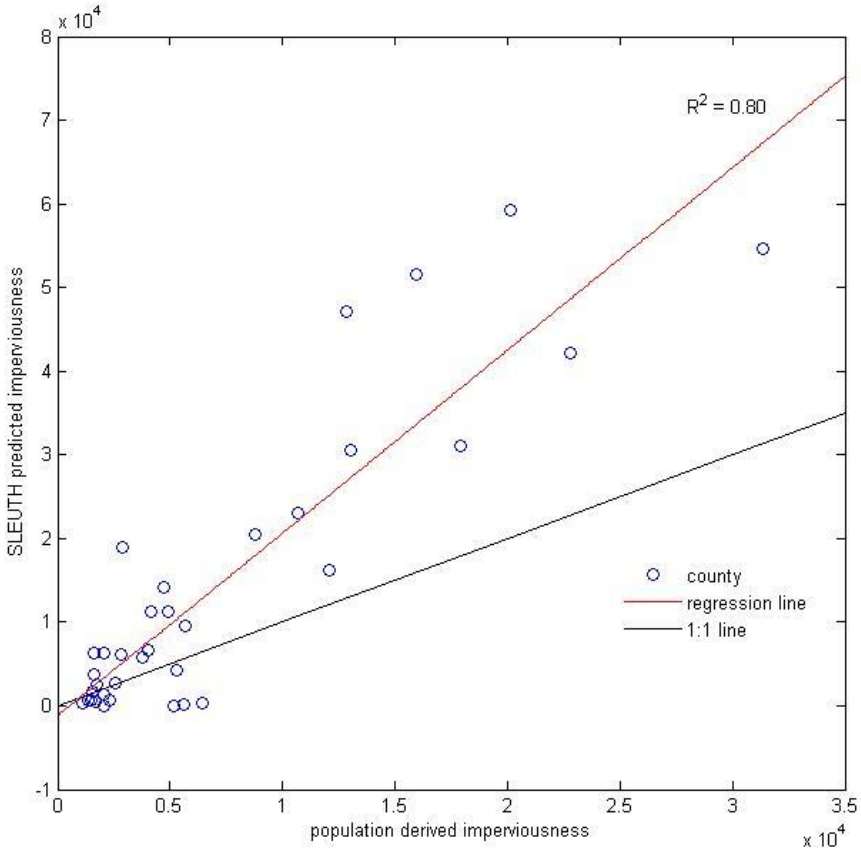

Figure 6. Comparison of population-derived impervious area and SLEUTH output for year 2050

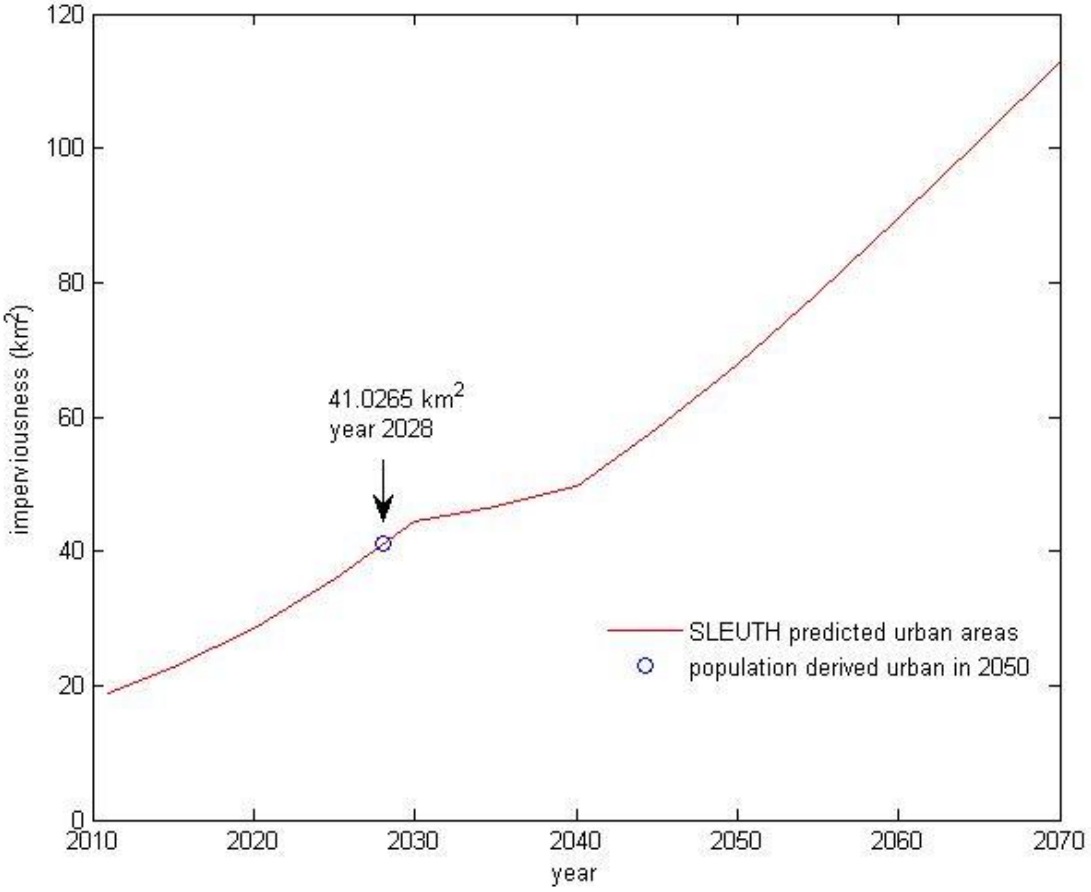

Figure 7. SLEUTH predicted impervious surface area from 2010 to 2070 for Stafford County, Virginia. Note Population-derived impervious surface area was 41.0265km^2 for year 2050.

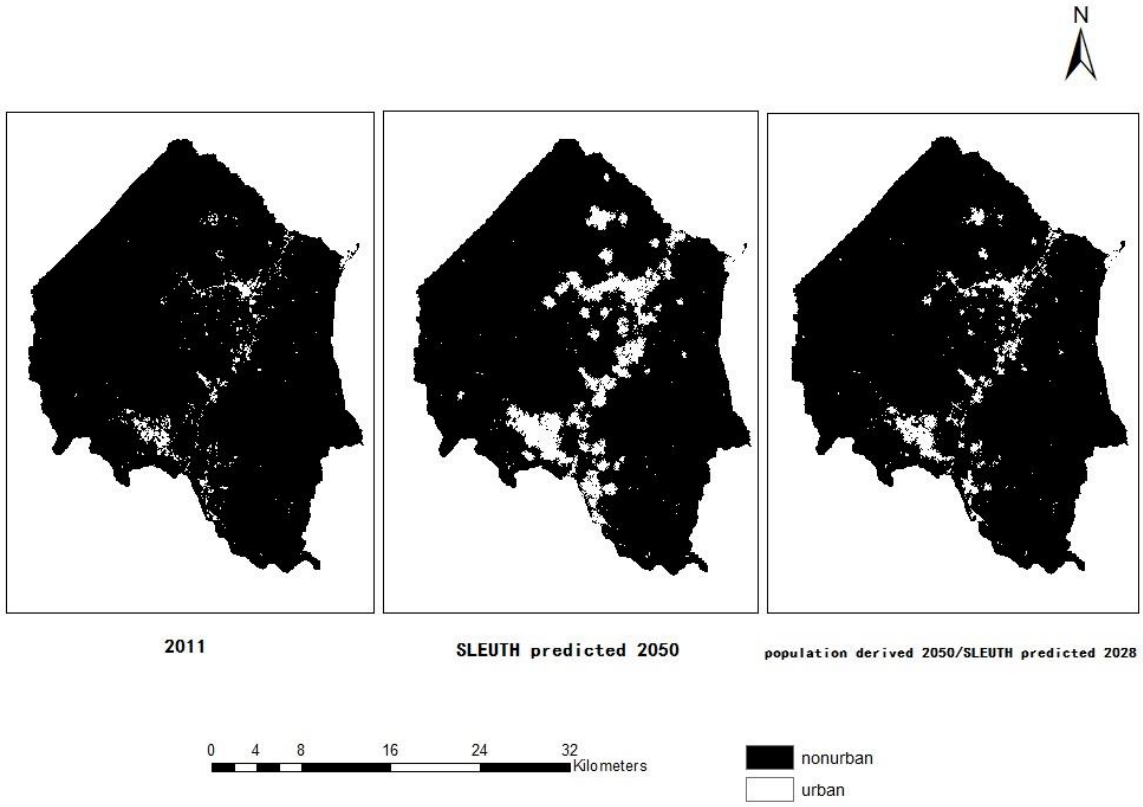

Figure 8. Comparison of NLCD impervious surface (2011) and SLEUTH predicted impervious surface area for year 2050 and 2028. Note Population-derived impervious surface area was 41.0265km^2 for year 2050 and the number matched SLUETH output of year 2028.

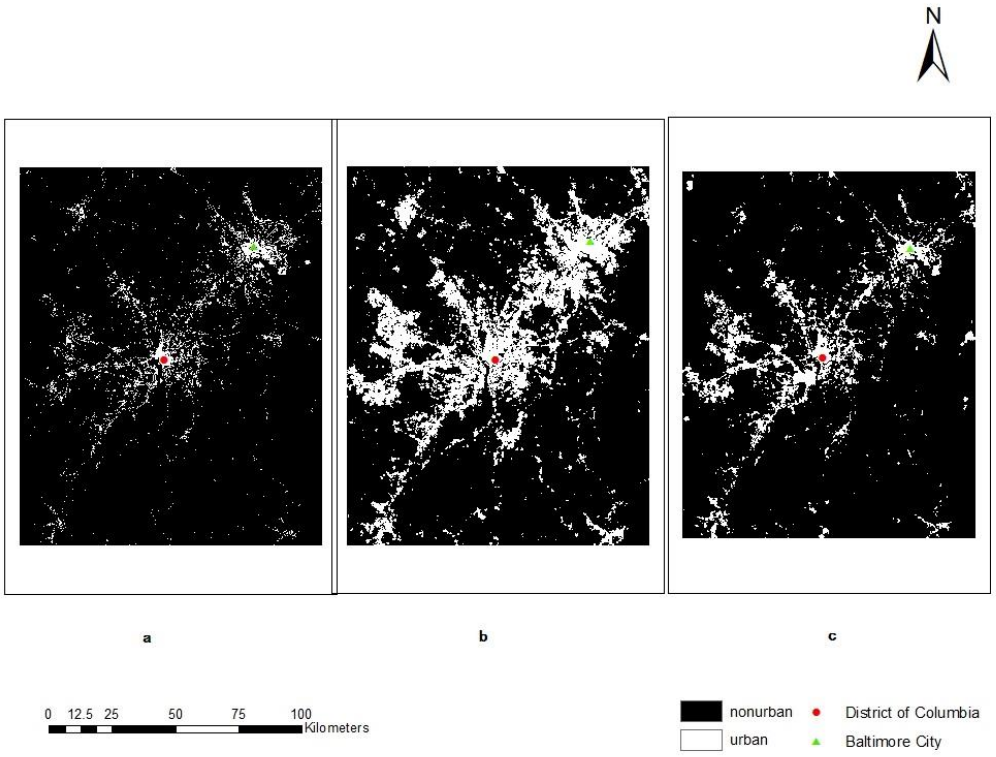

Figure 9. Urban areas for historical 1996(a), SLEUTH predicted 2050(b) and population-derived 2050(c)

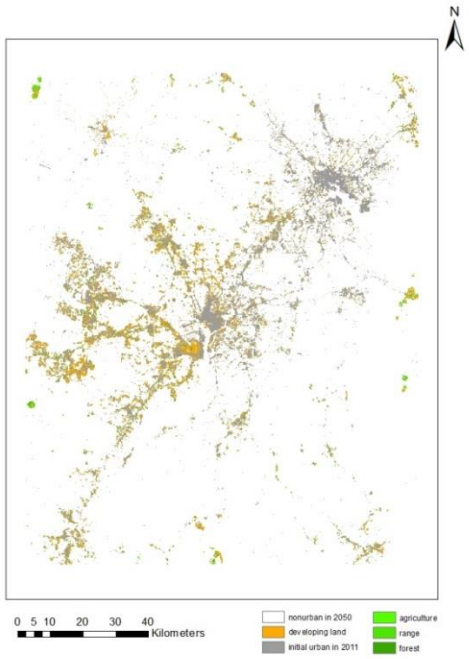

Figure 10. Distribution of landscapes transformed to urban in 2050

Table 1. Accuracy assessment for 2014 urban/nonurban classification

		reference			
		urban	nonurban	Total	User's accuracy (%)
modeled	urban	116961	50796	167757	69.7
	nonurban	60856	1993475	2054331	97.0
	Total	177817	2044241	2222088	
	Producer's accuracy (%)	65.8	97.5		Total accuracy (%) 94.9

Table 2. Accuracy assessment of changed pixels from 2011 to 2014

	reference			
	urban	Nonurban	Total	Accuracy (%)
Modeled changing pixels	13972	16366	30338	46.1

Table 3. Landscapes in 2011 transformed to urban in 2050

Land cover type	Developing lands	Urban	Agriculture	Range	Forest	Others
Transformed to urban (km^2)	536.4	996.3	20.4	17.9	75.1	22.6
Percentage (%)	32.14	59.71	1.22	1.07	4.50	1.35

Table 4. Landscape pattern metrics/indices for the years 2011 and 2050 (TA (Hectares) = Total Area, PN = patch number, MPS (Hectares) = mean patch size, LPI (%) = largest patch index, ED (Meters per hectare) = edge density, PAFRAC = Perimeter-Area Fractal Dimension)

Year	TA	NP	MPS	LPI	ED	PAFRAC
2011	105537	12013	8.7853	0.5897	10.3625	1.5568
2050	174973	8402	20.5633	1.9584	10.8038	1.4796